Calcif. Tissue Int. 32, 123-133 (1980)

Calcified Tissue International

Bone Cell Kinetics During Longitudinal Bone Growth in the Rat

Donald B. Kimmel and Webster S.S. Jee

Division of Radiobiology, Department of Pharmacology, University of Utah College of Medicine, Salt Lake City, Utah 84112, USA

Summary. The purpose of this work was to provide further knowledge about bone cell kinetics in the metaphysis of the growing long bone. Seventy rats were sacrificed from 1 to 120 h after injection of tritiated thymidine. Autoradiographs of 3 μm thick sections of the proximal tibial metaphysis were studied in a manner which allowed evaluation of labeled cell nuclei as a function of increasing age of metaphyseal tissue. A cell cycle duration study for osteoprogenitor cells was done. Labeled osteoprogenitor cells and osteoblasts first appeared at 1 h post-injection. The great majority of all labeled osteoprogenitor cells and osteoblasts was found within 1 mm of the growth cartilage-metaphyseal junction (GCMJ) at all times, apparently migrating with the moving GCMJ. In contrast, labeled osteoclast nuclei first appeared at 24 h post-injection within 0.3 mm of the GCMJ and remained always with the area of bone surface with which they were first associated, even as the GCMJ migrated away. By 5 days post-injection, the source of new labeled osteoclast nuclei in the metaphysis near the GCMJ was depleted, whereas that for the osteoblasts remained. The existence of two kinetically different, as well as ultrastructurally different, members of the metaphyseal osteoprogenitor cells population is postulated. A cell cycle time of 39 ± 18 h was found for the osteoprogenitor cell population, but has limited meaning. A schema for metaphyseal bone cell movements during longitudinal bone growth is presented.

Key words: Bone — Cell kinetics — Osteoprogenitor cell — Migration — Differentiation.

Send offprint requests to Dr. Donald B. Kimmel at the above address.

Introduction

Cell kinetics of bone cells in the metaphysis of the growing long bone was first investigated with tritiated thymidine (^{3}H-thymidine) 20 years ago in the proximal tibia of rats 6 weeks of age [1]. A similar study of the proximal tibial and rib metaphyses of 6-day-old rats was completed soon after [2]. The findings of these two studies, summarized below, now form the basis of current knowledge about bone cell kinetics in the metaphysis.

The authors agreed on the appearance, if not the name, of the principal proliferating bone cell (labeled with ^{3}H-thymidine 1 h after injection). Kember called it a mesenchymal cell, while Young preferred the name osteoprogenitor cell, because it implied some connection with bone cells. It was found most often within 0.5 to 1.0 mm of the growth cartilage-metaphyseal junction (GCMJ), located in the perivascular connective tissue between blood vessels and longitudinally oriented trabeculae of calcified cartilage. It was characterized by poorly visualized cytoplasm and a spindle-to-ovoid-shaped nucleus (Fig. 1).

Kember alone noted that, even though the growth cartilage was advancing at a rate of 0.125 mm/day at this site in his animals, the labeled osteoprogenitor cells were within 0.5 to 1.0 mm of the GCMJ for at least 7 days after ^{3}H-thymidine injection. He concluded that the osteoprogenitor cells were migrating in the metaphysis in the direction of bone elongation.

By studying animals sacrificed from 1 h to 28 days after ^{3}H-thymidine injection, both authors studied the differentiation of bone cells. Both found that a few osteoblasts took ^{3}H-thymidine label 1 h after injection and that the fraction of osteoblasts labeled began to climb after about 8 h. They concluded that the cause of this was an influx of cell nuclei which had acquired ^{3}H-thymidine label as osteoprogenitor cells.

0171-967X/80/0032-0123 $02.20

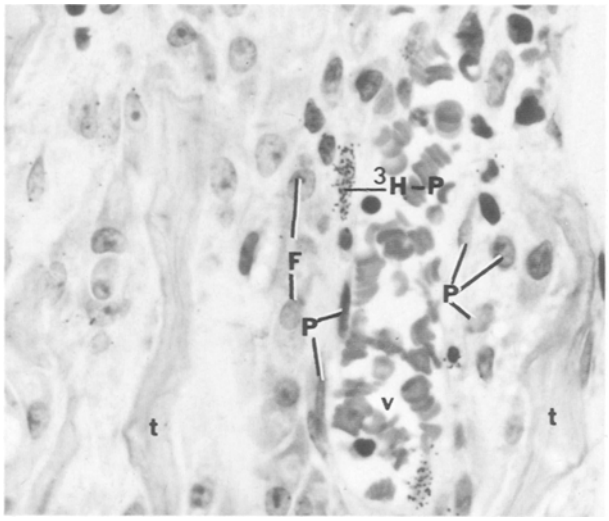

Fig. 1. Osteoprogenitor cell with ^{3}H-thymidine label. Typical osteoprogenitor cell *(3H-P)* with ^{3}H-thymidine label is seen between blood vessel *(v)* and longitudinal hard tissue trabeculae *(t)*. Numerous unlabeled osteoprogenitor cells *(P)* are also present. A number of osteoblasts *(F)* are present in this area taken from a 0.3 mm band at 1 h after injection of ^{3}H-thymidine. (550×, hematoxylin and eosin)

Although both agreed that no osteoclast nuclei were labeled with ^{3}H-thymidine at 1 h after injection, denying proliferative ability for nuclei of osteoclasts, there were other differences in their data concerning osteoclast nuclei. Kember noted that only a few ^{3}H-thymidine-labeled osteoclast nuclei ever appeared and that they were found in a random pattern with regard to time and region of appearance in the metaphysis. Young saw a more orderly pattern to their appearance. The first labeled ones appeared at 9 h after ^{3}H-thymidine injection, and more continued to appear until a maximum labeled fraction was reached at 45–50 h post-^{3}H-thymidine. A finding of Young that has gone unheralded is that he studied two metaphyseal zones, one just adjacent to and a second about 1 mm from the GCMJ. He noted that labeled osteoclast nuclei appeared in greater numbers sooner in the proximal zone than in the distal zone. He also found that the maximum labeled fraction for osteoclast nuclei was the same as the initial fraction labeled for osteoprogenitor cells and concluded that osteoclast nuclei, as well as osteoblasts, were descended from osteoprogenitor cells.

These authors conducted studies which allowed them to speculate on various aspects of the cell cycle. Kember's technique of continuous labeling with ^{3}H-thymidine suggested that the growth fraction of osteoprogenitor cells, the fraction actually in the proliferative cycle, was about 0.5. Young's fraction of labeled mitoses (FLM) study, interpreted first by a hand analysis method [3] and later by an automated method [4], gave a cell cycle time estimate of 33 ± 34 h for the metaphyseal osteoprogenitor cells.

Since the time of these two studies, pioneering ultrastructural work [5] identifying ^{3}H-thymidine-labeled metaphyseal osteoprogenitor cells of two types, "A-cells" of osteoclast/monocyte-like appearance, and "B-cells" of osteoblast-like appearance, has appeared and been confirmed [6]. In addition, there has been an explosion of technology, experiments, and knowledge about bone cells during the 1970's which is summarized in several reviews [7–10].

The purpose of this experiment is to apply autoradiographic techniques to thinner (3 μm) bone sections than were available to earlier investigators and to use a more exacting quantitative histologic technique for examination of aging metaphyseal tissue [11] to provide new data from an old model. The new data will be combined with other pertinent recent data to describe the cellular sequence of events during bone elongation.

Materials and Methods

Animals

Seventy 100-g male Sprague-Dawley rats were obtained from Hormone Assay Co. (Chicago, Ill.). They were caged five per 0.5 m^2 cage and permitted 7 days' acclimation to laboratory conditions [Wayne Lablox fed ad lib.; light cycle (8 a.m.–8 p.m. on); and 22°C at 40% humidity]. Their daily weights were recorded during this period. Rats exhibiting atypical growth patterns were excluded from the experiment. On the day when an individual rat first reached 170 g in weight, it was injected subcutaneously once with 0.5 μCi ^{3}H-thymidine per gram body weight (16.7 Ci/mM, New England Nuclear Co., Seattle, Washington). This dose of ^{3}H-thymidine is known to be nonradiotoxic as a cell label, even when followed for several weeks [12]. The rats were then killed in pairs, at 1, 2, 4, 6, 8, 10, 12, 16, 20, 24, 28, 32, 34, 36, 38, 40, 42, 44, 46, 48, 50, 52, 54, 56, 60, 70, 80, 90, 100, 110, and 120 h after ^{3}H-thymidine injection. Additional rats were killed singly at 0.5, 1.33, 1.67, 2.5, 3, 65, 75, and 85 h after ^{3}H-thymidine injection.

Histologic Procedures

The sections were prepared to the stage where they were ready to be stained as described previously [11]. At this point, in complete darkness, the slides were dipped in Kodak's NTB liquid emulsion (at 41°C) (LSB-1-4; Catalog# 165 4425; Eastman Kodak Co., Rochester, New York) and allowed to dry overnight in a low humidity atmosphere at 20°C. They were placed in bakelite boxes in light-tight cans at −18°C for selected exposure periods. Sections from animals sacrificed less than 8 h after ^{3}H-thymidine

injection were exposed for 15 days. Those from animals sacrificed 9 to 60 h after ^{3}H-thymidine injection were exposed for 30 days. Those from all others were exposed for 60 days. This was to compensate for the potential dilution of ^{3}H-thymidine label of individual nuclei caused by cell division. At the end of the exposure period, the slides were developed in D-19 and fixed in Fixer (Eastman Kodak Catalog#'s 146 4593 and 197 1746, Rochester, New York), then rinsed 30 min in running cold tap water. Staining and mounting was then completed [11]. It is noted that the pH of the hematoxylin was lowered with citric acid to minimize staining of the gelatin base of the autoradiographic emulsion. This procedure was quite helpful in increasing the ability to identify individual cells more accurately.

Technique of Microscopic Analysis

At least two sections from each animal were selected. Prior to starting the analysis, each slide was given a code which obscured its identity from the reader. The criteria previously established for cell identification [11] were applied here. A labeled cell nucleus was considered one with three or more autoradiographic grains directly over it.

1. AGE-RELATED TISSUE. For this work, only the sections of paired animals sacrificed at 1, 12, 24, 36, 48, 60, 70, 80, 90, 100, 110, and 120 h after injection of ^{3}H-thymidine were selected. A technique of microscopic examination of metaphyseal tissue of increasing age similar to that applied in the previous paper [11] was employed here. A magnification of about 850× (oil immersion) which allowed easy identification of autoradiographic grains was used. Bands of tissue 0.2 mm high, with centers at 0.3, 0.7, 1.1, 1.5, 1.9, 2.3, 2.7, and 3.1 mm from the GCMJ were selected for data analysis. The exact data collected in each field were numbers of: unlabeled osteoblasts, labeled osteoblasts, unlabeled osteoprogenitor cells, labeled osteoprogenitor cells, unlabeled osteoclast nuclei, and labeled osteoclast nuclei.

2. CELL CYCLE ANALYSIS. This examination was confined to the area where most mitotic metaphyseal osteoprogenitor cells were found, that within 0.5 mm of the GCMJ. All such tissue, from cortex to cortex, was examined for the numbers of unlabeled interphase osteoprogenitor cells, labeled interphase osteoprogenitor cells, unlabeled mitotic osteoprogenitor cells, and labeled mitotic osteoprogenitor cells. This work generally required five or six sections from each animal to give the necessary 100 total mitotic figures.

Data Processing

1. AGE-RELATED TISSUE. The average age of the tissue in each band is calculated by dividing the distance from the GCMJ by the growth rate. The raw data listed above were stored in a Data General Eclipse S/130 minicomputer. The following values were calculated:

a. *Fraction of all ^{3}H-thymidine-labeled metaphyseal nuclei of one type located in areas of particular age* ($F_{d(\text{cell type})t}$). For example, if, at 48 h post-^{3}H-thymidine, there were 100 labeled osteoprogenitor cell nuclei in the eight bands examined, and 60 were in the 0.3 mm band, this number ($F_{0.3(OPC)48}$) would be 0.6, for the 0.3 mm band.

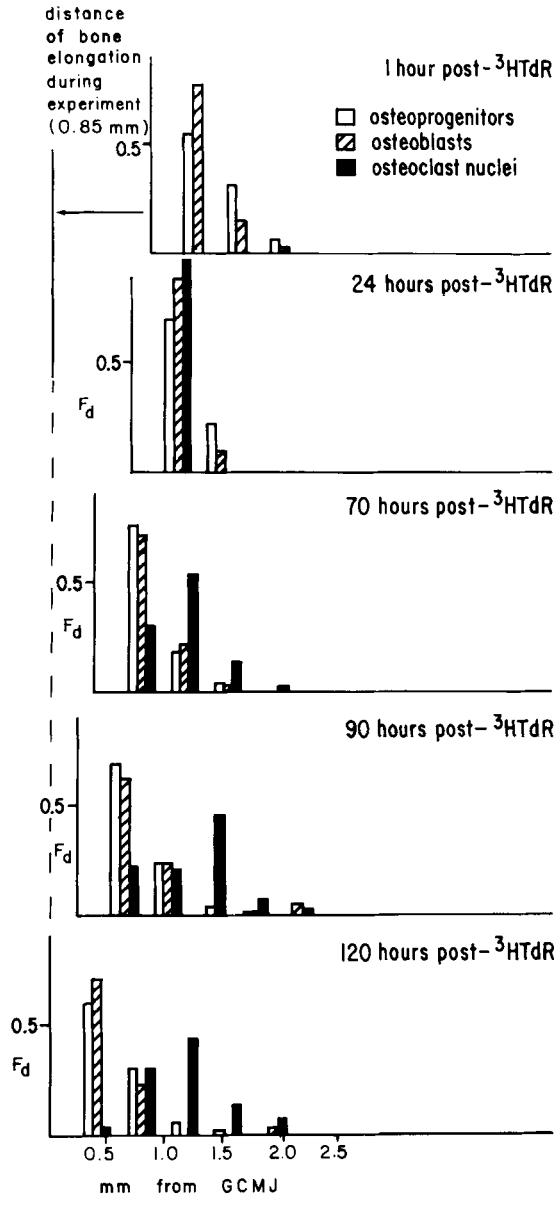

Fig. 2. Fraction of all ^{3}H-thymidine-labeled metaphyseal nuclei of one type located in areas of particular age. At 1 h after injection of ^{3}H-thymidine, about 60% of all labeled osteoprogenitor cells are in the first band, 30% are in the second band, and 10% are in the third band

b. *Median location of labeled nuclei of one type*. This is calculated from the following formula:

$$d = \frac{\sum_{0.3}^{3.1} d\, F_{d(\text{cell type})t}}{0.3}$$

For example, if 0.6 of the labeled cells of one type were located at 0.3 mm and the rest at 0.7 mm, the median location would be 0.46 mm from the GCMJ.

c. *Fraction of all nuclei of a particular type in the two youngest bands labeled with ^{3}H-thymidine*. For example, if there were 600 osteoprogenitor cells in these two bands, 90 of which were labeled, this number would be 0.15.

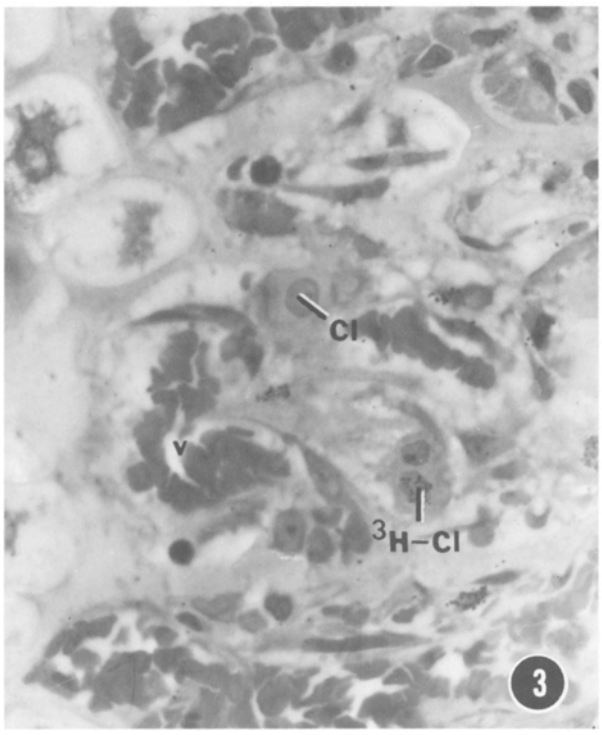

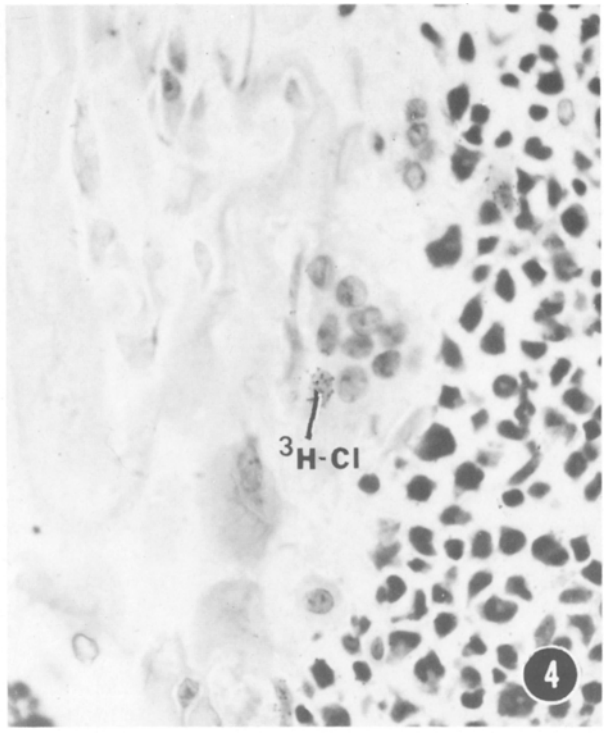

Fig. 3. Metaphyseal tissue adjacent to GCMJ from rat killed 12 h after injection of ^{3}H-thymidine. Irregular outline of GCMJ (*at left*) delimited by last closed cartilage lacunae adjacent to the metaphysis is seen. ^{3}H-thymidine-labeled osteoclast nucleus (*^{3}H-Cl*) is seen. Other osteoprogenitor cells (*P*) and osteoclasts (*Cl*) are seen in this area characterized by many blood vessels (*v*). (350×, hematoxylin and eosin)

Fig. 4. Metaphyseal tissue of 1.5 mm band from rat killed 5 days after injection of ^{3}H-thymidine. Osteoclast with one ^{3}H-thymidine-labeled nucleus (*^{3}H-Cl*) is present at the bone surface in this relatively aged region of the metaphysis. (550×, hematoxylin and eosin)

d. *Fraction of all ^{3}H-thymidine-labeled nuclei represented by the ^{3}H-thymidine-labeled nuclei of one type*. For example, if there were 200 labeled nuclei in the metaphysis, 120 of which were osteoprogenitor cells, this number would be 0.6 for the osteoprogenitor cells.

2. Cell Cycle Analysis. The raw data above collected from each animal were submitted to computer analysis by an automatic method [13].[1] The method compares the submitted data on labeled mitoses and interphase cells to values of labeled mitoses and interphase cells that are predicted for populations with known values of the following cell cycle parameters:

T_c, the cell cycle duration; T_s, the duration of DNA synthesis phase; T_{G1}, the duration of G1 phase; T_{G2}, the duration of G2 phase; T_m, the duration of mitosis; GF, the growth fraction, or fraction of cells which are actually in the mitotic or proliferative cycle.

Results

1. Age-Related Tissue

a. *Fraction of all ^{3}H-thymidine-labeled metaphyseal nuclei of one type located in areas of particular age* ($F_{d(\text{cell type})t}$) (Fig. 2). Only five post-injection periods (1, 24, 70, 90, and 120 h) are shown in the figure, but the histograms are demonstrative of the data from all animals. At all times from 1 h to 5 days after ^{3}H-thymidine injection, the labeled osteoprogenitor cells and labeled osteoblasts are found relatively near the GCMJ. In stark contrast to this, the osteoclast nuclei display a very different pattern. At 1 h post-^{3}H-thymidine, there are no labeled osteoclast nuclei anywhere in the bands studied. By 1 day post-^{3}H-thymidine, some appear, all of which are located in the youngest tissue studied (Fig. 3). By 70 h, the labeled osteoclast nuclei are spread over the first four bands, about half of them being found in the 0.7 mm band. By 90 h post-^{3}H-thymidine, the maximum is in the 1.1 mm band, and at 120 h, the maximum remains in that region, but the fraction in the 0.3 mm band decreases to almost zero, whereas that in the 1.5 and 1.9 mm bands increases (Fig. 4). The data suggest that the labeled osteoclast population and the GCMJ grow further apart as time after ^{3}H-thymidine injection increases.

b. *Median location of labeled nuclei of one type* (Fig. 5). This was characterized with respect to time after the injection of ^{3}H-thymidine. From the linear

[1]The authors gratefully acknowledge the help of Gerald Vattuone and Dr. Mortimer Mendelsohn of Lawrence Livermore Laboratory.

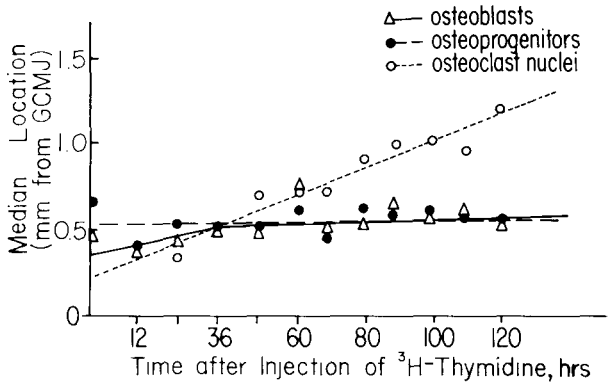

Fig. 5. Median location of labeled nuclei of each type. Linear regression analysis values are found in Table 1

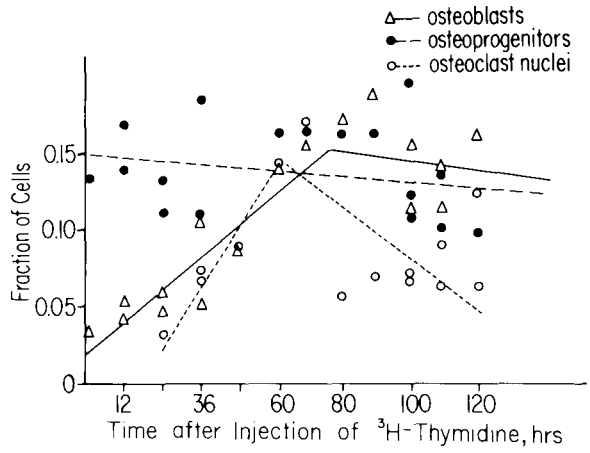

Fig. 6. Fraction of all nuclei of a particular type in the two youngest bands which are labeled with ^{3}H-thymidine. Values for linear regression analyses are listed in Table 1

regression analysis, it is concluded that the slope of neither the osteoblast nor the osteoprogenitor cell line was significantly different from zero, indicating that their position in the metaphysis relative to the GCMJ does not change over the 5-day period. In the same way, it is concluded that the slope of the osteoclast nucleus line is highly significantly different from zero ($P < 0.001$), with a value of 0.0063 mm/h or 0.151 mm/day, similar to the growth rate at this center.

c. *Fraction of all nuclei of a particular type in the two youngest bands labeled with ^{3}H-thymidine* (Fig. 6). The fraction of osteoprogenitor cells labeled initially is about 0.15 and does not change significantly throughout the study. The fraction of osteoblasts initially labeled was about 0.02; it rises to about 0.15 between 1 and 70 h ($P < 0.001$), then does not change significantly over the remainder of the study. Wide variation in the data may mask the fact that the number of labeled nuclei in the youngest areas of the metaphysis does diminish by 3 days and longer after injection of ^{3}H-thymidine (Fig. 2).

d. *Fraction of all ^{3}H-thymidine-labeled nuclei represented by the ^{3}H-thymidine-labeled nuclei of one type* (Fig. 7). The fraction of labeled cell nuclei which is osteoprogenitor cells drops from about 0.6 one hour post-^{3}H-thymidine to 0.2 by 5 days post-^{3}H-thymidine ($P < 0.001$). Conversely, the fraction which is osteoblasts rises from 0.4 to 0.6 ($P < 0.001$) over the same period. The fraction which is osteoclast nuclei is zero at 1 h, then rises from 0.02 at 24 h to 0.2 by 5 days post-^{3}H-thymidine ($P < 0.025$).

2. Cell Cycle Analysis

The fraction of labeled mitoses curve which best fits

Table 1. Linear regression analyses from Figures 3–5

Cell type	Slope	y_i	R	Slope different from zero ($P<$)
Figure 3				
Osteoprogenitor cells	−0.00024	+0.152	0.38	No
Osteoblasts				
1–70 h	+0.0018	+0.017	0.91	0.001
60–120 h	−0.0002	+0.172	0.17	No
Osteoclast nuclei				
24–70 h	+0.0029	−0.034	0.97	0.005
60–120 h	−0.0008	+0.18	0.45	No
Figure 4				
Osteoprogenitor cells	−0.0018	+0.597	0.96	0.001
Osteoblasts	+0.0011	+0.395	0.91	0.001
Osteoclast nuclei	+0.00056	+0.024	0.73	0.025
Figure 5				
Osteoprogenitor cells	+0.0003	+0.45	0.18	No
Osteoblasts	+0.0012	+0.37	0.55	No
Osteoclast nuclei	+0.0063	+0.22	0.96	0.001

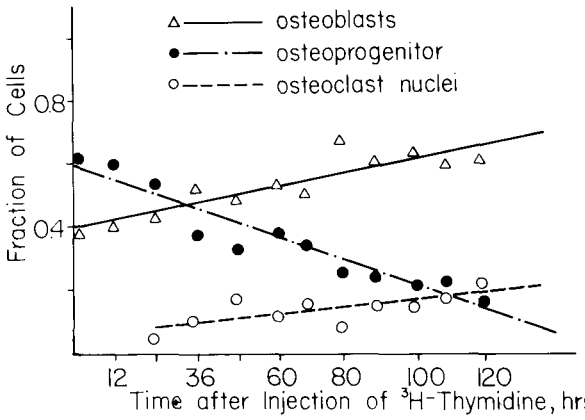

Fig. 7. Fraction of all labeled nuclei represented by labeled nuclei of one type. Values for linear regression analyses are found in Table 1

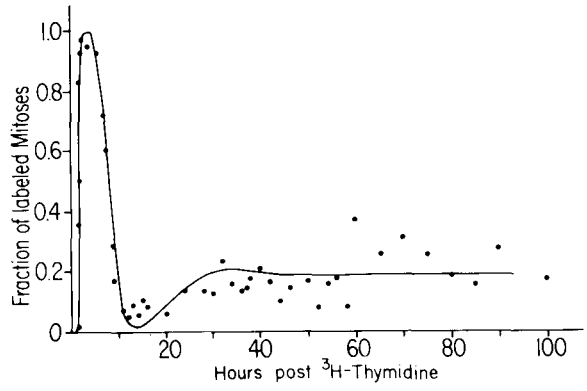

Fig. 8. Fraction of labeled mitoses curve for osteoprogenitor cells. This curve was iteratively fitted by the computer program to FLM curves with known values for phase durations. The best fit values are seen in Table 2

the rendered data is shown in Figure 8. The data on cell cycle phase durations which are derived from that curve are listed in Table 2.

Discussion

The purpose of this work was to attempt to further previous work [1, 2] by using technical advances of thinner sections and orderly analysis of metaphyseal tissue, to make for more accurate identification of both cells and regions of tissue. The data are interpreted in light of more recent data which have contributed to the understanding of bone cell lineage and function.

Among the data of Kember and Young confirmed in this study are (a) the eventual accumulation of ^{3}H-thymidine-labeled osteoblasts and osteoclast nuclei in the same fraction as the original osteoprogenitor cell ^{3}H-thymidine-labeled fraction, (b) the migration of some osteoprogenitor cells along trabeculae in the direction of bone elongation, and (c) the ^{3}H-thymidine-labeling of osteoblasts at 1 h after injection of ^{3}H-thymidine.

Table 2. Cell cycle phase durations and growth fraction for osteoprogenitor cells

Phase	Duration (h)	Coefficient of variation
T_c	38.9	0.45
T_s	6.5	0.2
T_{G1}	30.5	0.57
T_{G2}	1.1	0.27
T_m	1.0	0.28
GF	0.9	0.2

The most striking new finding of the current study is the difference in metaphyseal osteoblast and osteoclast kinetics. Such a difference was suggested but not clearly defined in Young's data. Once ^{3}H-thymidine-labeled nuclei are incorporated into osteoclasts in young metaphyseal tissue, the labeled nuclei (hence, the osteoclasts) remain associated with the same region of trabecular hard tissue, even as the GCMJ grows away, for at least 5 days. The osteoclasts and the bone seem to age together. In addition, the source of ^{3}H-thymidine-labeled osteoclast nuclei is nearly depleted by 5 days post-^{3}H-thymidine, whereas that for the osteoblasts persists.

Although individual osteoblasts probably also remain with the trabeculae with which they are initially associated, this phenomenon is masked since labeled nuclei are lost from identification as osteoblasts as they either become incorporated into bone as osteocytes or lose histologic features which identify them as osteoblasts (i.e., Golgi body, basophilic cytoplasm). The appearance of a few labeled members in the osteoprogenitor cell/osteoblast populations in lower regions of the metaphysis at 5 days post-^{3}H-thymidine is representative of this second possibility. In addition, whereas the source of ^{3}H-thymidine-labeled osteoclast nuclei in new metaphyseal tissue is nearly depleted by 5 days after injection of ^{3}H-thymidine, that for the ^{3}H-thymidine-labeled osteoblasts in new metaphyseal tissue persists.

The most likely explanation for these findings is that, although both osteoblasts and osteoclast nuclei are spawned by the light microscopic osteo-

progenitor cell population, they arise from two kinetically different, as well as ultrastructurally different (5), subpopulations in the metaphyseal osteoprogenitor cell population. In one subpopulation, that for the osteoclasts, all labeled members, with or without cell division, eventually are incorporated as nuclei into osteoclasts. In the other, that for the osteoblasts, ^{3}H-thymidine is incorporated, the cell divides, then one daughter cell becomes an osteoblast and the other migrates along the trabeculum in direction of bone elongation, to supply new metaphyseal tissue with osteoprogenitor cells for osteoblasts.

This understanding has great implications for study of cell cycle times in bone cells. First, the metaphysis remains the major place where sufficient mitoses are present to make an FLM study possible in a steady-state bone cell model. Even at this, by cell kinetic standards, the study is difficult, being limited to autoradiography and relatively arduous FLM analysis. Second, no cell cycle time study of preosteoclasts would ever be possible because there is no repeated division of labeled cells, a necessity in FLM studies. Third, the results of this study (39 ± 18 hours) and Young's (33 ± 34 h) take on dubious meaning because the ^{3}H-thymidine-labeling of both preosteoclasts and preosteoblasts was studied, prior to the disappearance of labeled preosteoclasts. Fourth, the lower variability of the current study may be happenstance due to technical improvements of sectioning and autoradiography, but is surely not due to study of a pure osteoprogenitor cell population. A study of pure preosteoblasts might finally yield a well-defined T_c for proliferating bone cells. There is reason to hope that cell cycle analysis of relatively pure populations of bone cells from the calvaria of fetal rats could yield meaningful results, when done by the method of flow microfluorimetry [14].

An interesting difference in the current data and that of Young is that he first found ^{3}H-thymidine-labeled osteoclast nuclei after 9 h, whereas the current study did not detect such cells until 24 h after injection of ^{3}H-thymidine. Young's data are correct; he studied the youngest metaphyseal tissue, that just adjacent to the GCMJ, whereas the youngest tissue characterized by the current data is some 0.2–0.4 mm from the GCMJ, about 1.8 days of age. The site of initial labeling of osteoclast nuclei is most likely the youngest metaphyseal tissue (Fig. 3). The cells then remain stationary as the GCMJ grows away, placing them within range of the data collection procedure of this study by 24 h post-injection.

It is suggested that the GCMJ is the initial site of appearance of new osteoclasts or precursors in the metaphysis. Studies of resorption-defective osteopetrotic mice done some years ago support this idea. When osteopetrotic mice were in either permanent or temporary parabiotic union with normal littermates, the first site where resorption returned toward normal was just beneath the GCMJ in the growing long bones [15, 16]. The inference is that competent osteoclasts arrived at this site first in the osteopetrotic animals, just as did the ^{3}H-thymidine-labeled ones in the normal animals of the current study.

Kember's data suggest the presence of small numbers of ^{3}H-thymidine-labeled osteoprogenitor cells at 1 mm and further into the metaphysis 5 to 14 days after injection of ^{3}H-thymidine. This trend emerges again in the current data. The source for such cells is not clear, but may represent (a) ^{3}H-thymidine-labeled nuclei released from osteoclasts, (b) released osteocytes previously labeled with ^{3}H-thymidine while osteoprogenitor cells or osteoblasts, or (c) cells now identified as osteoprogenitor cells, which went through an osteoblastic phase, then entered a resting phase at the bone surface, never becoming buried in bone as osteocytes. Since the cells appear in tissue 1.1 to 1.5 mm from the GCMJ, 7 to 10 days of growth time has elapsed. This may be somewhat short for osteoclast nucleus lifespan, and quite probably very short for the duration of the osteoprogenitor cell-osteoblast-osteocyte release sequence. The resting osteoblast explanation seems most acceptable.

It has been suggested that osteocyte nuclei released by osteoclastic bone resorption are a source of new osteoclast nuclei [17, 18]. However, the data clearly show that the initial site of appearance of labeled nuclei in osteoclasts is near the GCMJ, which is coincidentally a site of little bone and hence, few osteocytes. With few osteocytes available in this region, it is doubtful that they could be a source for osteoclast nuclei. Although this indirect reasoning does not rule out the released osteocyte nucleus as a source for osteoclast nuclei, other more likely pathways are clearly present in this model.

Some years ago, it was suggested that monocytes were the precursors of osteoclast nuclei [19]. More recently, it has been shown that monocytes themselves can bring about bone resorption [20, 21]. The kinetic behavior of preosteoclasts and osteoclasts in the growing long bone metaphysis provides additional evidence that they are related to the mononuclear phagocyte series. For review, the mononuclear phagocyte series is divided into three groups of cells: the marrow residents, promon-

ocytes; the bloodstream residents, monocytes; and the tissue residents, mononuclear phagocytes [22, 23]. The sequence of events in the life of a mononuclear phagocyte is listed. Promonocytes synthesize DNA, divide, then within as little as 2 h release their progeny to the bloodstream as monocytes. Monocytes, cells on the way from marrow to tissue with a mean transit time of 32 h, are not DNA-synthesizing cells. Following an injection of ^{3}H-thymidine, the monocyte population is initially unlabeled but is subsequently composed of heavily labeled members, released from marrow after one post-^{3}H-thymidine promonocyte division, and lightly labeled ones, released from marrow after two or more post-injection divisions. Following a ^{3}H-thymidine injection, a few labeled mononuclear phagocytes appear within 1 h. Significant numbers appear at 18–24 h after injection and then nearly disappear by about 72–96 h post-^{3}H-thymidine [24]. These kinetics bear some similarity to the sequence of appearance of labeled osteoclast nuclei in the zone nearest the GCMJ, where none are present at the start, some begin to appear by 10 h, a maximum appears at 60–70 h, and most disappear by 100+ h. It is possible that ^{3}H-thymidine label in preosteoclasts of this study was caused by either or both (a) incorporation of ^{3}H-thymidine in DNA-synthesizing preosteoclasts, or (b) delivery to tissue from the bloodstream of monocytes of the heavily labeled type. Either source would provide for the incorporation of labeled nuclei into osteoclasts as seen in this study. It is most likely true that monocytes provide a continuous flow of new mononuclear phagocytes to the tissue of the GCMJ region, but at 50 h (1.5 times the mean transit time from marrow to tissue) or more after ^{3}H-thymidine injection, the lack of label would indicate that they are mainly from the lightly labeled monocyte population. Their labeling is then of such low intensity that, despite the lengthened periods of autoradiographic exposure employed for long-term animals, they are no longer detectable as labeled cells. This coincides with the description of labeling seen in the tissue nearest the GCMJ.

^{3}H-thymidine-labeled osteoblasts 1 h after injection have been seen repeatedly [1, 2, 25–27]. The explanation for this may now be clearer than it has been in the past. A group of experiments relying on mitotic figure counts [28] or grain counts [25] had reached the conclusion that, in these cells, ^{3}H-thymidine incorporation was associated with the synthesis of metabolic DNA and not with cell replication. An elegantly designed experiment, using the jejunal crypt model of Appleton, superceded the quantitative problems of grain counts, cell counts, and mitotic figure counts, and proved beyond a reasonable doubt that every crypt cell taking up ^{3}H-thymidine divides within 12 h [29]. Although that work has not been repeated for bone cells, it seems reasonable to believe that osteoblasts would follow basic cell proliferation rules. Furthermore, there are several examples of tissues in which individual cells both proliferate and make structural or enzyme proteins, as would osteoblasts in dividing and synthesizing new bone matrix simultaneously. These include antibody-producing cells [30], pigmented retinal cells [31], rat heart ventricle cells [32], cultured chondrocytes [33], parotid gland cells [34], and erythrocytes [35]. Certainly there are exceptions to all rules, but this indirect line of reasoning is presented in an attempt to characterize osteoblasts as a typical functional population with some proliferative ability, especially in a zone where the need for both new cells and new bone tissue is great.

These findings about bone cell behavior during bone elongation are of interest to hard tissue radiobiologists and may explain an observed paradox. Following single injections of bone-seeking radioisotopes like ^{239}Pu, osteosarcoma development shows a predilection for trabecular bone. This is true for both growing and adult animals. If radiation decays striking proliferating bone cells is a critical event in the induction of osteosarcoma, one might expect this predilection to be accentuated near the ends of growing long bones in beagles, where proliferative bone cells abound. However, there is no extra tendency for osteosarcoma development near the ends of growing long bones in such animals [36], when compared to young adult animals. This cell kinetics study provides a possible answer. First, highly proliferative osteoprogenitor cells are constantly moving into new metaphyseal tissue, which contains relatively little nuclide when compared to older bone present at the time of injection. The cells, although still proliferative, have a smaller chance to be struck by a radiation decay than if they had stayed in old tissue. Second, proliferative preosteoclasts divide once and become incorporated into osteoclasts where they are nonproliferative, and represent little risk for cancer induction, even though they remain in old, nuclide-laden tissue. Third, only osteoblasts of low proliferative potential remain in old tissue where nuclide concentration is high, and they are likely to become incorporated into bone, where their proliferative life also ends.

It is wise to summarize at this point by tying the current data to those produced in the past in an attempt to deduce the most likely sequence of events surrounding cell proliferation in the metaphysis of a growing long bone (Fig. 9). The principal proliferating bone cells of the metaphysis are osteo-

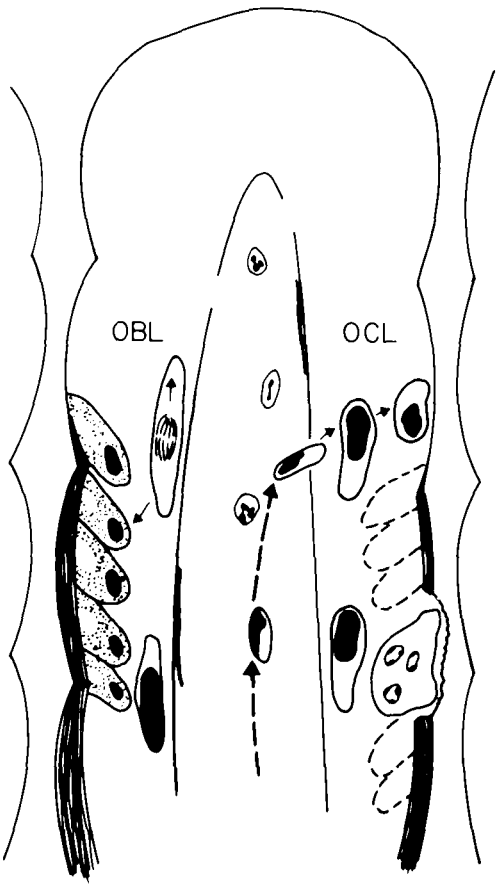

Fig. 9. Conceptual representation of bone cell population kinetic behavior during bone elongation. The growth cartilage-metaphyseal junction (GCMJ) is at the top of the figure. A pair of longitudinal calcified cartilage septae with an intervening blood vessel and perivascular tissue is depicted. The preosteoblast-osteoblast population at the left of the blood vessel shows a mitotic cell which will send one cell migrating in the direction of bone elongation and the other to be an osteoblast. The preosteoclast-osteoclast nucleus population at the right shows a monocyte arriving in the tissue as a mononuclear phagocyte, then transforming to or joining a pre-existing osteoclast, with or without cell division. In actuality, the populations are not on separate sides of the blood vessel, but function while intermingled

progenitor cells, located mainly within 1 mm of the GCMJ and between blood vessels and calcified longitudinal septae of hard tissue (cartilage and bone) [1, 2]. There are two types of such osteoprogenitor cells, which are intermingled and indistinguishable with the light microscope, but which are readily identified under fairly low power electron microscopic examination (10,000-15,000×) [5]. The first is preosteoclasts, which are cells similar in appearance to monocytes, which are loaded with mitochondria and free ribosomes, as are osteoclasts. They also have considerable phagocytic ability [6]. The second is preosteoblasts, which are cells with a large amount of rough endoplasmic reticulum and a poorly developed Golgi body. These properties suggest that differential dye staining of relatively thin (1 μm) sections of metaphyseal tissue may allow identification of the two types without electron microscopy in the future.

The preosteoclasts are actually the bone equivalent of the mononuclear phagocyte of other soft tissues which also possess proliferative capabilities under some conditions in the liver [37, 38], the lung [39], and the peritoneum [40-42]. They are deposited in the tissue as circulating monocytes, which enter the metaphysis through blood vessel pores just adjacent to the GCMJ [43, 44]. The evidence for blood vessel delivery of preosteoclasts to bone is supported directly by a number of studies [44-52], but direct delivery from hematopoietic cells via migration through bone marrow cannot be excluded. Although in this position, the preosteoclast may either synthesize DNA and divide and have both daughter cells incorporated into osteoclasts, or join an osteoclast without proliferation. The osteoclasts thus formed are stationary in the metaphysis, as the GCMJ moves away, maintaining an association with one region of hard tissue. Their fate is uncertain, but it is possible that their lifespan is approximately equal to that of the trabecula with which they are initially associated, which is about 3 weeks (3.5 mm/(0.17 mm/day)) or 20.5 days.

In contrast, preosteoblasts migrate along trabeculae with the velocity of bone elongation. Each division gives one daughter to become an osteoblast and one to migrate and maintain the preosteoblast population in tissue added to the metaphysis by the degeneration of transverse septae to cause opening of cartilage lacunae. Osteoblasts themselves have both proliferative and matrix synthesis functions in this area of high cell recruitment and new matrix synthesis. Although many osteoblasts are encased in bone subsequent to their period of osteoid synthesis [1, 53], it seems possible that a few remain at the bone surface and resume the appearance of osteoprogenitor cells at longer times after their initial labeling.

References

1. Kember, N.F.: Cell division in endochondral ossification. A study of cell proliferation in rat bones by the method of tritiated thymidine autoradiography, J. Bone Joint Surg. [Br.] **42**:824-839, 1960
2. Young, R.W.: Cell proliferation and specialization during endochondral osteogenesis in young rats, J. Cell Biol. **14**:357-370, 1962

3. Quastler, H., Sherman, F.G.: Cell population kinetics in the intestinal epithelium of the mouse, Exp. Cell Res. **17**:420–438, 1959
4. Kember, N.F.: Cell population kinetics of bone growth: the first ten years of autoradiographic studies with tritiated thymidine, Clin. Orthop. Rel. Res. **76**:213–231, 1971
5. Scott, B.L.: Thymidine-^{3}H electron microscope radioautography of the osteogenic cells in the fetal rat, J. Cell Biol. **35**:115–126, 1967
6. Thyberg, J.: Electron microscopic studies on the uptake of exogenous marker particles by different cell types in the guinea pig metaphysis, Cell Tissue Res. **156**:301–315, 1975
7. Hall, B.K.: The origin and fate of osteoclasts, Anat. Rec. **183**:1–11, 1975
8. Gothlin, G., Ericsson, J.L.E.: Review of ultrastructure, origin, and function of the osteoclast, Clin. Orthop. Rel. Res. **120**:201–231, 1976
9. Jee, W.S.S., Kimmel, D.: Bone cell origin at the endosteal surface. In P. Meunier (ed.): Bone Histomorphometry, pp. 113–131. Paris, Armour, 1978
10. Owen, M.: Histogenesis of bone cells, Calcif. Tissue Res. **25**:205–207, 1978
11. Kimmel, D., Jee, W.S.S.: A histomorphometric study of the metaphysis of the growing long bone, Calcif. Tissue Int. (accepted)
12. Cleaver, J.: Thymidine Metabolism and Cell Kinetics. John Wiley, New York, 1967
13. Takahashi, M., Hogg, J.D., Mendelsohn, M.L.: The automatic analysis of FLM curves, Cell Tissue Kinet. **4**:505–518, 1971
14. Gray, J.W.: Cell cycle analysis of perturbed cell populations. Computer simulation of sequential DNA distributions, Cell Tissue Kinet. **9**:499–516, 1976
15. Walker, D.G.: Congenital osteopetrosis in mice cured by parabiotic union with normal siblings, Endocrinology **91**:916–920, 1972
16. Walker, D.G.: Osteopetrosis cured by temporary parabiosis, Science **180**:875, 1972
17. Messier, B., Leblond, C.P.: Cell proliferation and migration as revealed by radioautography after injection of thymidine-^{3}H into male rats and mice, Am. J. Anat. **106**:247–285, 1960
18. Tonna, E.A.: An electron microscopic study of osteocyte release during osteoclasis in mice of different ages, Clin. Orthop. Rel. Res. **87**:311–317, 1972
19. Fischman, D.A., Hay, E.D.: Origin of osteoclasts from mononuclear leucocytes in regenerating newt limbs, Anat. Rec. **143**:329–335, 1962
20. Mundy, G.R., Altman, A.J., Gondel, M.D., Bandell, J.G.: Direct resorption of bone by human monocytes, Science **196**:1109–1111, 1977
21. Kahn, A.J., Stewart, C.C., Teitelbaum, S.L.: Contact-mediated bone resorption by human monocytes in vitro, Science **199**:988–990, 1978
22. Meuret, G.: Origin, ontogeny, and kinetics of mononuclear phagocytes, Adv. Exp. Med. Biol. **73**(pt.A):71–81, 1978
23. van Furth, R.: Origin and kinetics of monocytes and macrophages, Semin. Hematol. **7**:125–141, 1970
24. Volkmann, A.: The origin and turnover of mononuclear cells in peritoneal exudates in rats, J. Exp. Med. **124**:241–253, 1966
25. Owen, M., McPherson, S.: Cell population kinetics of an osteogenic tissue, II, J. Cell Biol. **19**:33–42, 1963
26. Simmons, D.J.: Cellular changes in the bones of mice as studied with tritiated thymidine and the effects of estrogen, Clin. Orthop. Rel. Res. **26**:176–189, 1963
27. Simmons, D.J., Kunin, A.S.: Autoradiographic and biochemical investigations of the effect of cortisone on the bones of the rat, Clin. Orthop. Rel. Res. **55**:201–215, 1967
28. Appleton, T.C., Pelc, S.R., Tarbit, M.H.: Formation and loss of DNA in intestinal epithelium, J. Cell Sci. **5**:45–55, 1969
29. Burholt, D.R., Schultze, B., Maurer, W.: Autoradiographic confirmation of the mitotic division of every mouse jejunal crypt cell labeled with ^{3}H-thymidine, Cell Tissue Kinet. **6**:229–237, 1973
30. Makela, O., Nossal, G.J.V.: Autoradiographic studies on the immune response. II. DNA synthesis amongst single antibody-producing cells, J. Exp. Med. **115**:231–243, 1962
31. Cahn, R.D., Cahn, M.B.: Heritability of cell differentiation: clonal growth and expression of differentiation in retinal pigment cells *in vitro*, Proc. Natl. Acad. Sci. U.S.A. **55**:106–113, 1966
32. Mark, G.E., Strasser, F.F.: Pacemaker activity and mitosis in cultures of new born rat heart ventricle cells, Exp. Cell Res. **44**:217–233, 1966
33. Cahn, R.D., Lasher, R.: Simultaneous synthesis of DNA and specialized cellular products by differentiating cartilage cells *in vitro*, Proc. Natl. Acad. Sci. U.S.A. **58**:1131–1138, 1967
34. Redman, R.S., Sreebny, L.M.: Proliferative behavior of differentiating cells in the developing rat parotid gland, J. Cell Biol. **46**:81–87, 1970
35. Campbell, G LeM., Weintraub, H., Mayall, B.H., Holtzer, H.: Primitive erythropoiesis in early chick embryogenesis. II. Correlation between hemoglobin synthesis and the mitotic history, J. Cell Biol. **50**:669–681, 1971
36. Bruenger, F.W., Stevens, W., Stover, B.J., Taylor, G.N., Smith, J.M., Buster, D.S., Atherton, D.R.: The distribution and pathological effects of Pu-239 in beagles exposed as juveniles, Radiat. Res. (submitted)
37. Edwards, J.L., Klein, R.E.: Cell renewal in adult mouse tissues, Am. J. Pathol. **38**:437–453, 1961
38. North, R.J.: Cellular kinetics associated with the development of acquired cellular resistance, J. Exp. Med. **130**:299–314, 1962
39. Shorter, R.G., Titus, J.L., Divertie, M.B.: Cell turnover in the respiratory tract, Dis. Chest **46**:138–142, 1964
40. Forbes, I.J., Mackaness, G.B.: Mitosis in macrophages, Lancet **2**:1203–1204, 1963
41. Wiener, E.: DNA synthesis in peritoneal mononuclear leucocytes, Exp. Cell Res. **45**:450–459, 1967
42. North, R.J.: The mitotic potential of fixed phagocytes in the liver as revealed during the development of cellular immunity, J. Exp. Med. **130**:315–326, 1969
43. Schenk, R.K., Wiener, J., Spiro, D.: Fine structural aspects of vascular invasion of the tibial epiphyseal plate of growing rats, Acta Anat. (Basel) **69**:1–17, 1968
44. Andersen, H., Matthiessen, M.E.: The histiocyte in human fetal tissues: its morphology, cytochemistry, origin, function, and fate, Z. Zellforsch. **72**:193–202, 1966
45. Buring, K.: On the origin of cells in heterotopic bone formation, Clin. Orthop. Rel. Res. **110**:293–302, 1973
46. Gothlin, G., Ericsson, J.L.E.: On the histogenesis of the cells in fracture callus, Virchows Arch. [Zellpathol.] **12**:318–329, 1973

47. Walker, D.G.: Bone resorption restored in osteopetrotic mice by transplants of normal bone marrow and spleen cells, Science **190:**784–785, 1975
48. Walker, D.G.: Spleen cells transmit osteopetrosis in mice, Science **190:**785–786, 1975
49. Allyn, P.G., Minkin, C.: Origin of the osteoclast: studies with a quail-mouse chimera, J. Dent. Res. **55:**B219, 1976
50. Kahn, A.J., Simmons, D.J.: Investigations of cell lineage in bone using a chimera of chick and quail embryonic tissue, Nature **258:**325–327, 1975
51. Simmons, D.J., Kahn, A.J.: Cell lineage in fracture healing in chimeric bone grafts, Calcif. Tissue Int. **27:**247–253, 1979
52. Marks, S.C., Jr.: Osteopetrosis in the *ia* rat cured by transfusion of spleen cells from a normal littermate, J. Dent. Res. **55:**B202, 1976
53. Owen, M. Cell population kinetics of an osteogenic tissue I, J. Cell Biol. **19:**19–32, 1963

Received November 19, 1979 / Revised March 5, 1980 / Accepted March 5, 1980